Micro-Coaxial Impedance Transformers

Negar Ehsan, *Member, IEEE*, Kenneth J. Vanhille, *Member, IEEE*, Sébastien Rondineau, *Member, IEEE*, and Zoya Popović, *Fellow, IEEE*

***Abstract*—This paper demonstrates two broadband air-filled micro-coaxial 4:1 (2–24 GHz) and 2.25:1 (2–22 GHz) impedance transformers. The 4:1 transformer converts 50 to 12.5 Ω and the 2.25:1 device transforms 50 to 22.22 Ω. The circuits are fabricated on silicon with PolyStrata technology, and are implemented with 650 μm × 400 μm air-filled micro-coaxial lines. Back-to-back circuits and single structures with geometrical tapers are designed for systematic characterization. Simulation and measurement results are in excellent agreement. The return loss for both transformers is better than 15 dB over the design bandwidth.**

***Index Terms*—Coaxial components, coaxial transmission lines, impedance matching, transformers.**

I. Introduction

A transmission line transformer (TLT) with frequency-independent characteristics was first introduced in 1944 by Guanella [1]. These devices transform current, voltage and impedance like conventional wire-wound transformers, but are implemented with interconnected transmission lines [2]. Fig. 1(a) shows the transmission-line model of a 4:1 impedance transformer, where two equal-length equal-delay lines are connected in a way that imbalances currents in the outer conductors so that energy is transmitted via a transverse transmission-line mode [3], [4]. Because the shield of one line is connected to the inner conductor of the other equal-length line, the currents add in phase at the low-impedance end. As a result of the equal delay, the transformation becomes theoretically independent of the line length, and therefore frequency independent. In 1959, Ruthroff introduced a new TLT class that uses only one transmission line and thus is considerably smaller than the Guanella transformer. However, it is not theoretically frequency independent [2].

Coaxial TLTs are widely used as impedance matching networks for broadband power amplifiers in the UHF and VHF ranges [3]. For frequencies under 100 MHz, transformers are constructed from pairs of wire wound around ferrite cores. At UHF and low microwave frequencies, coaxial lines are used in transformer implementation. They are commonly ferrite-loaded to increase the inductance, thereby increasing the electrical length of the transmission lines and decreasing the low-frequency cutoff. At microwave frequencies, planar configurations with multi-layer printed circuit boards and monolithic microwave integrated circuit structures have also been demonstrated [3], [5], [6].

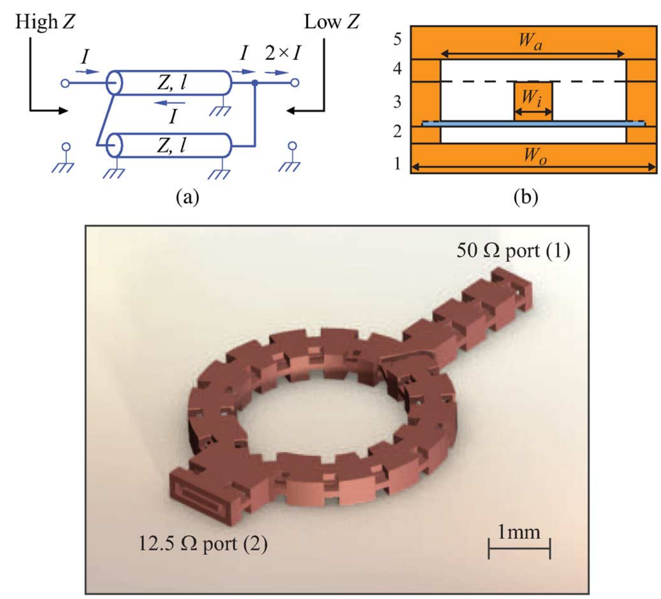

Fig. 1. (a) Transmission line model of 4:1 Guanella transformer. (b) Cross section of the five-layer line, where layers 1, 3, and 5 are 100 μm tall and layers 2 and 4 are 50 μm tall. The inner conductor is supported by 18-μm-thick and 100-μm-wide dielectric straps. (c) Rendering of the 4:1 Guanella transformer implemented in the five-layer PolyStrata environment.

In this paper, we use PolyStrata wafer-scale technology to design Guanella-type broadband micro-coaxial TLTs from 2 to above 24 GHz. Both narrowband and broadband components such as resonators, couplers, antennae, and broadband Wilkinson dividers have been demonstrated with this process [7]–[10]. Air-filled micro-coaxial lines implemented with this technology have distinct advantages for broadband miniature high-frequency circuits, which are summarized as follows:

- very low loss (e.g., 0.1 dB/cm measured at 38 GHz [11]);
- excellent isolation enabling miniaturization (60-dB measured isolation at Ka band for neighboring lines sharing a common ground wall [12]);
- low dispersion up to high frequencies enabling broadband component design [13];

Manuscript received April 04, 2010; revised June 26, 2010; accepted June 30, 2010. Date of publication October 21, 2010; date of current version November 12, 2010. This work is funded by the Defense Advanced Research Projects Agency (DARPA) DMT program, U.S. Army contract W15P7T-07-C-P437.

N. Ehsan was with the Department of Electrical, Computer, and Energy Engineering, University of Colorado, Boulder, CO 80309 USA. She is now with the NASA Goddard Space Flight Center, Greenbelt, MD 20771 USA (e-mail: negar.ehsan@nasa.gov).

K. J. Vanhille is with Nuvotronics, LLC, Radford, VA 24141 USA (e-mail: kvanhille@nuvotronics.com).

S. Rondineau is with Solentech, Rio Grande do Sul, 90020-080, Brazil (e-mail: sebastien.rondineau@gmail.com).

Z. Popović is with the Department of Electrical, Computer, and Energy Engineering, University of Colorado, Boulder, CO 80309 USA (e-mail: zoya@colorado.edu).

Color versions of one or more of the figures in this paper are available online at http://ieeexplore.ieee.org.

Digital Object Identifier 10.1109/TMTT.2010.2078410

- a wide range of possible characteristic impedances fabricated in the same process, enabling design flexibility [14];
- excellent control of dimensions over a large area enabling precise device optimization.[1]

This paper addresses the following topics.

- Section II discusses the fabrication process and outlines the characteristics of the 4:1 Guanella transformer and its bandwidth capabilities. In particular, we explain the design procedure and full-wave electromagnetic implementation of this transformer in the 2–24 GHz range.
- Section III presents the 4:1 impedance transformer and its performance in three different environments (air, air-cavity, and silicon).
- Section IV demonstrates a 2.25:1 impedance transformer, its design procedure, full-wave analysis, and implementation. The prototype performance is compared with full-wave simulation results.

One of the main goals of this study is to demonstrate a compact broadband matching circuit. The TLT shown in Fig. 1(c) is 6 mm long, which is over an order of magnitude shorter than a tapered line with similar return loss at 2 GHz.

II. 4:1 Impedance Transformer Fabrication and Design Procedure

The Guanella-type transformer as shown in Fig. 1(a) consists of two transmission lines with a series connection at the high-impedance end and parallel connections at the low-impedance end. For a 4:1, 50 Ω to 12.5 Ω transformer, the impedance of the transmission line sections is $\sqrt{Z_{\text{low}} \times Z_{\text{high}}} = 25\ \Omega$. The low impedance is motivated by the application discussed at the end of the paper; 12 Ω is a close match to the ≈ 10-Ω input and output impedances of a broadband GaN traveling-wave amplifier.

A. Fabrication

The fabrication process involves sequential deposition of copper layers and photoresist on a silicon wafer. Copper layer thicknesses can range from 10 to 100 μm, with gap-to-height and width-to-height aspect ratios of 1:1.2 and 1:1.5, respectively. Fig. 1(b) shows the cross section of a five-layer 50-Ω micro-coaxial line, in which layers 1, 3, and 5 are 100 μm tall and layers 2 and 4 are 50 μm tall. The inner conductor is supported by 100-μm-long dielectric straps with 700-μm periodicity. After the desired layers have been deposited, the photoresist is removed ("released") through 200 μm × 200 μm release holes (which have 700-μm periodicity) on layers 1, 2, 4, and 5. The characteristic impedances available for a micro-coaxial line with this specific layer configuration range from 8 to 54 Ω [14].

B. Design Procedure

An ideal transformer, as described in Section I, has infinite bandwidth, regardless of the length of the transmission lines and the geometry of the interconnects. However, in practice,

[1]Nuvotronics, available [online]: http://nuvotronics.com/designGuidlines.php

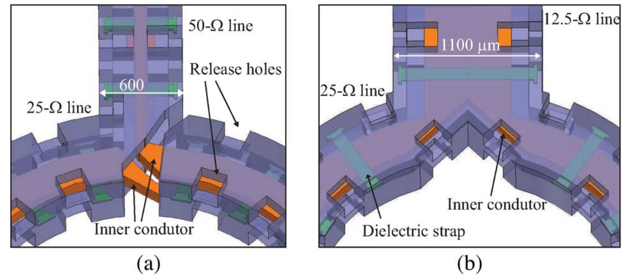

Fig. 2. (a) Series interconnection between the 25 Ω line and 50 Ω line; (b) parallel interconnection between the 25-Ω line and 12.5-Ω line.

the design of a TLT for microwave frequencies between 2 and 24 GHz requires careful full-wave electromagnetic (EM) simulations; Ansoft's High-Frequency Structure Simulator (HFSS) is used in this study. Fig. 1(c) shows the 4:1 micro-coaxial transformer designed to be implemented in the five-layer process described above. The important design features are the lengths of the lines and the geometrical details of the interconnections between the transmission lines at the series and parallel junctions. The lengths of the transmission lines contribute to both the lower and upper frequency limits. The lower frequency limit is directly proportional to the reactance associated with the inductance of the middle section transmission lines. For a given transformer design that operates between f_1 and f_2, in order to extend the low-frequency limit to $(f_1 - \Delta f_1)$, the electrical lengths of the transmission lines should be increased. However, this will also result in a shift in the high-frequency limit to $(f_2 - \Delta f_2)$. For example, if $f_1 = 2$ GHz and $f_2 = 24$ GHz, to change the lower frequency limit to 1 GHz, we would increase the length of the two transmission lines to $[f_1/(f_1 - \Delta f_1)]l$. However, this would shift f_2 down by some Δf_2, where $\Delta f_2 > \Delta f_1 = 1$ GHz. In order to maintain the high-frequency limit at f_2, the junctions need to be re-optimized. For the design presented here, a length of $l \approx 5$ mm is chosen for the desired bandwidth of at least 2–24 GHz. The second important factor that sets the upper frequency limit is the parasitic reactance associated with each transmission-line junction.

Fig. 2(a) shows the series interconnection between the middle section transmission lines and the 50-Ω transmission line. This region is designed such that it produces the lowest possible inductance and capacitance parasitics with the given design rules for gaps between the conductors and widths of the conductors. Fig. 2(b) shows the parallel interconnection between the middle section transmissions lines and the 12.5-Ω transmission line. The chamfer at the junction of this interconnection is designed such that it creates a smoother transition from the two 25-Ω lines to the 12.5-Ω line; as a result, the upper frequency limit increases.

To illustrate the importance of full-wave analysis and interconnect optimization, Fig. 3 shows simulation results when the transmission line interconnections are not optimized, for two obvious rectangular and circular geometries. The circular geometry improves the performance even without optimized junctions, since it contains fewer discontinuities, and reduces coupling. Fig. 4 shows the simulation results of a transformer with the circular geometry after extensive simulations to minimize

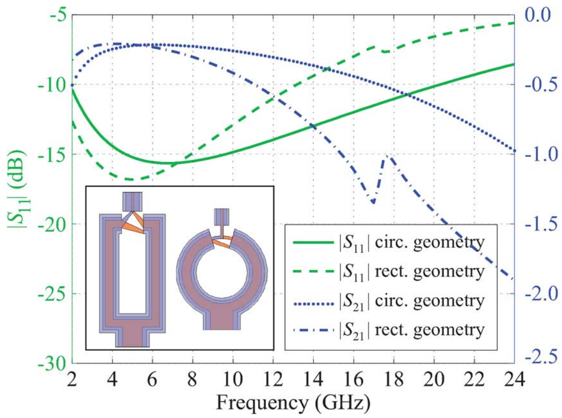

Fig. 3. S-parameter simulation results for two unoptimized 4:1 impedance transformers with circular and rectangular geometries. The simulations do not include release holes and dielectric straps.

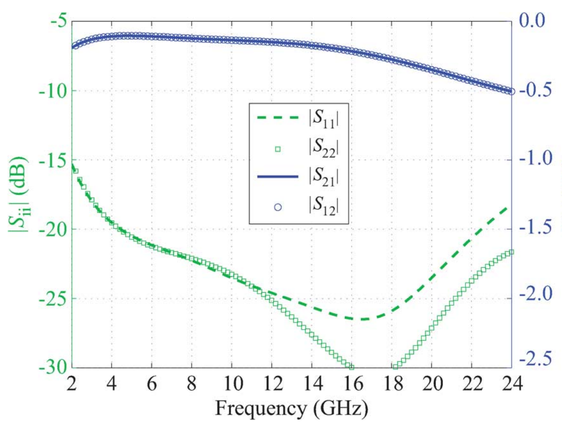

Fig. 4. Simulation results of the 4:1 circular impedance transformer, where the intraconnections are optimized for low parasitics. This simulation takes into account all the fabrication design rules including release holes and dielectric straps.

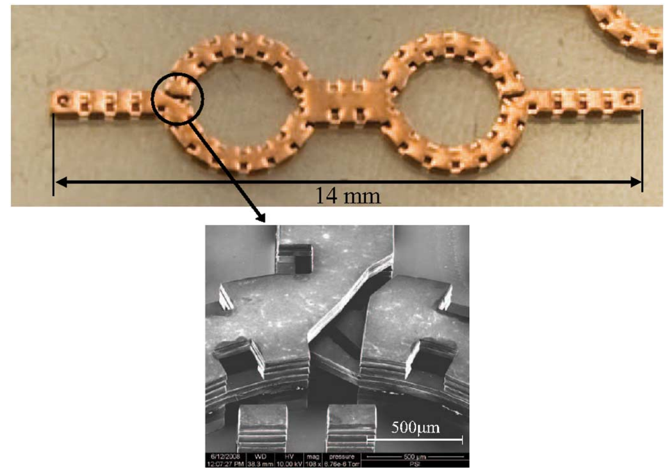

Fig. 5. Photograph of the 4:1 impedance transformer, fabricated in the PolyStrata. The micrograph on the bottom shows the photo of the fabricated intra-transformer connections between the 50-Ω and 25-Ω lines.

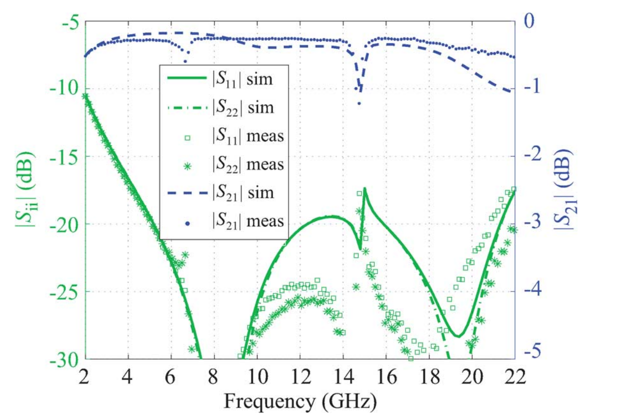

Fig. 6. Simulation and measured results of back-to-back 4:1 impedance transformers.

parasitics. $|S_{21}|$ for the optimized circular geometry transformer at 17 GHz is about 0.25 dB, whereas for the unoptimized circular and rectangular geometries it is 0.5 and 1.25 dB, respectively.

III. 4:1 Impedance Transformer Characterization

Because there is an imbalanced current on the outer conductors of a TLT, and an opening at the transmission-line connection, the environment around the TLT significantly affects its performance. The initial design discussed in the previous section is for the case of a transformer in air. However, in order to integrate the transformer with other components in a system, mechanical stability requires integration with a substrate or package. For this reason, in addition to the native silicon substrate, we investigate an air-filled metal cavity designed to function as a support for the transformer.

In this section, characterization of fabricated transformers in air (on foam, >99% air), air-filled metal cavity, and on a silicon substrate, is presented. In order to measure the transformer in a 50-Ω system, we considered two measurement methods: 1) a back-to-back structure and 2) a geometrical taper to connect the 12.5-Ω side of the transformer to a 50-Ω port. The former is done for a TLT designed in air and measured on foam and for a TLT designed and measured on a brass fixture with an air cavity beneath the intraconnections. The latter is discussed for the TLT designed and measured on a silicon substrate.

A. Micro-Coaxial Transformer in Air

Back-to-back transformers fabricated on a high resistivity silicon substrate, connected to each other at their 12.5 Ω ports (Fig. 5), allow measurements in a 50-Ω system. The circuit can be detached from the wafer and used as a free-standing device. A 5-mm-thick piece of foam ($\epsilon_r \approx 1.005$ at rf) is used for mechanical support. Measurements are performed with an Agilent E8364B network analyzer, Cascade Microtech 250-μm-pitch CPW microwave probes, and a Cascade Summit 9000 probe station. Calibration is performed with a set of on-wafer TRL calibration standards including two line lengths in order to cover the bandwidth [14]. Fig. 6 shows the measured and simulated results of the back-to-back transformers measured on foam. The small dip at 7 GHz is due to calibration, since the transition frequency between the two line standards is 7 GHz. The dip at 15 GHz, however, is due to a slight difference in electrical length of the two lines of each transformer.

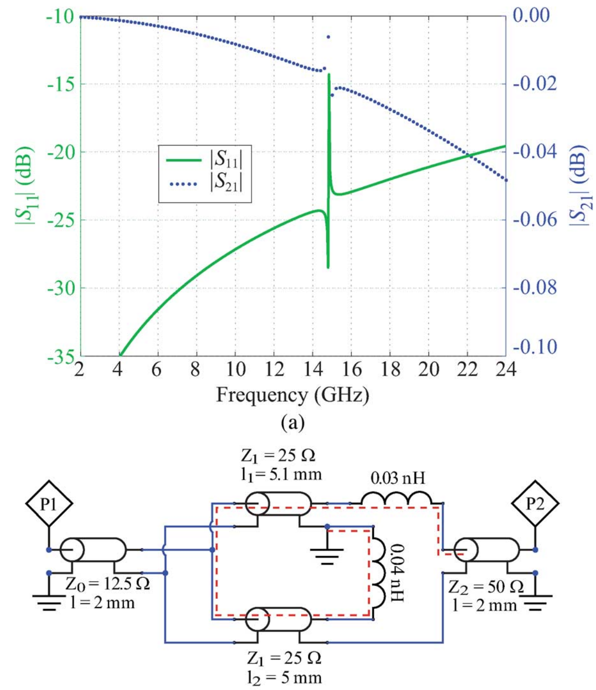

Fig. 7. (a) Circuit simulation results for a 4:1 transformer with 100-μm-length difference between the two transmission lines. (b) Circuit model including the parasitics at the 50-Ω junction. The coaxial transmission lines in this circuit model are ideal, so there is no limitation on the low frequency limit. The difference in line length causes the resonances at 15 GHz.

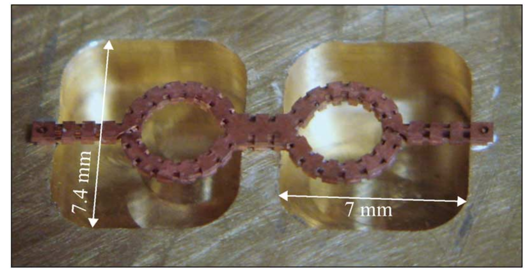

Fig. 8. Photograph of the back-to-back 4:1 transformer epoxied to the brass fixture. The depth of the cavities is 2.5 mm.

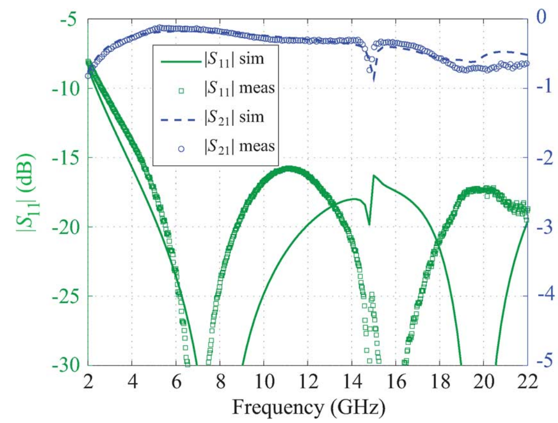

Fig. 9. Simulation and measured results of the back-to-back 4:1 impedance transformers on the brass fixture of Fig. 8.

Fig. 7(a) shows circuit simulations for a 100-μm-length difference corresponding to the bend of the left-hand line in Fig. 2(a). These results point to the importance of careful design of the connection between the transmission lines, where in addition to parasitics, any effective length differences need to be compensated. Specifically, in the circuit shown in Fig. 7(b), the two 25-Ω transmission lines create a $\lambda/2$ resonator indicated in the dashed line, causing a resonance at 14.8 GHz. In FEM simulations, this may not be obvious since it can depend on meshing, so the mesh should be varied to check for this effect.

B. Cavity-Backed Micro-Coaxial Transformer

For a TLT in air, a brass frame is designed for support as shown in Fig. 8. Since a micro-coaxial TLT operates based on current flow on the outer conductor as well as the inner conductor of the coaxial line, the surrounding frame could interfere with the operation of the transformer and degrade the performance. The perimeter and the depth of the structural support were simulated to find the optimal dimensions, where the depth of each cavity is approximately 2.5 mm ($\lambda/60$ at 2 GHz), and the sides are 7 and 7.4 mm in length.

Fig. 9 shows the simulated and measured results of the 4:1 back-to-back transformers placed on the brass structure, calibrated with a two-port short-open-load-through implemented in CPW on an alumina substrate, in the absence of an appropriate TRL calibration standard. This calibration method removes the effects of the cables and probes up to the probe tips. As shown in Fig. 9, the performance of the device is very similar to the one measured on foam. The only difference is that the standing wave shown in $|S_{11}|$ is slightly shifted to the left, due to a calibration difference.

C. Micro-Coaxial Transformer on Silicon

As mentioned in Section I, in order to enhance the lower frequency limit of TLTs, ferrite-loaded transmission lines or ferrite cores are commonly used. The ferrites increase the distributed inductance of the lines, and as a result, they are effectively longer and thus reduce the lowest operation frequency. In this case, the silicon substrate has a similar effect as ferrites; it reduces the lowest operation frequency at the cost of greater insertion loss. The dielectric increases the distributed capacitance between the two shield conductors in proportion to ϵ_r, and so their electrical length increases. The additional loss is due to coupling to substrate modes which are excited at the transmission-line intraconnections at the 50-Ω junction.

In the previous section, we showed the simulated and measured results of a back-to-back transformer, which are very similar to each other. However, the back-to-back structure does not show the transformation of 50 to 12.5 Ω. In order to demonstrate the 4:1 transformation for a single transformer on silicon, we added a 0.5-mm-long taper at the 12.5-Ω port that geometrically connects a 12.5-Ω line to a 50-Ω line. Fig. 10(a) shows the fabricated transformer with the taper on silicon, and (b) shows a sketch of the taper. The geometrical taper allows us to measure the transformer with the same micro-coax to CPW transition and 250-μm-pitch probes; however, due to its short length, it does

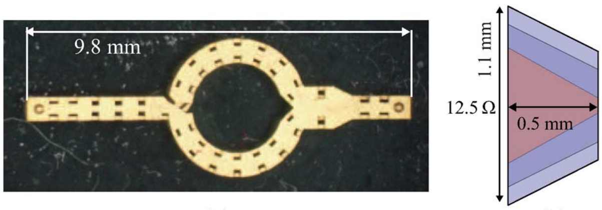

(a) (b)

Fig. 10. (a) Photograph of the single transformer on silicon with geometrical taper. (b) Detail of the geometrical taper connecting the 12.5-Ω line to 50-Ω line.

not actually transform 12.5 to 50 Ω. An estimation of the input impedance of the taper looking from the 50-Ω side at 12 GHz is

$$Z_{\text{in}} = Z_0 \frac{Z_L + \jmath Z_0 \tan(\beta l)}{Z_0 + \jmath Z_L \tan(\beta l)} = 12.68 + \jmath 5.9\ \Omega \qquad (1)$$

where $Z_0 = 50\ \Omega$, $Z_L = 12.5\ \Omega$, and $l = 0.5$ mm. Fig. 11(a) shows the simulation and measurement results of the 4:1 TLT measured with the 50 Ω system when the taper is not de-embedded. Since the geometrical taper does not have a significant effect on the output impedance, the taper can be de-embeded by normalizing the output port's impedance to 12.5 Ω. Fig. 11(b) shows the measured and simulated de-embedded results for this transformer.

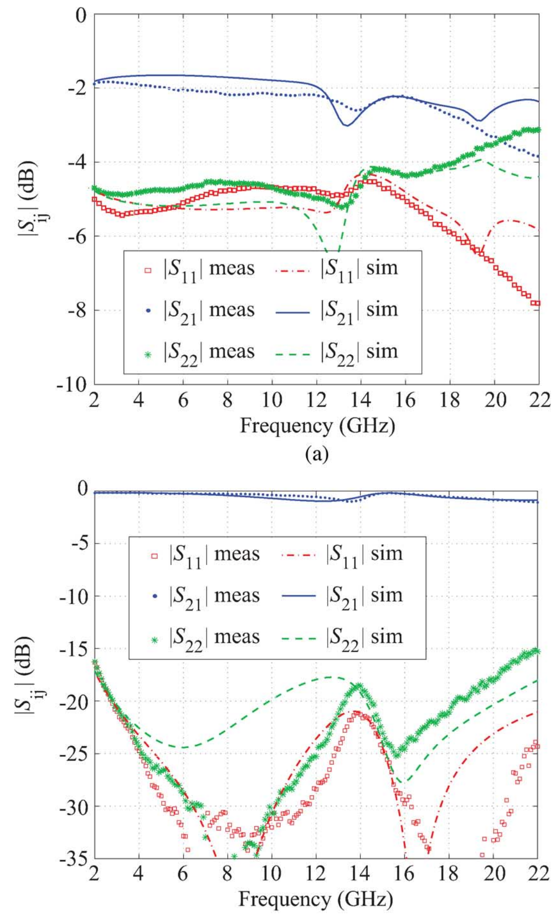

(b)

Fig. 11. (a) Simulated and measured results of a 4:1 transformer with geometrical taper on silicon. The geometrical taper is included in both simulation and measurement. (b) Simulated and measured results of a 4:1 transformer on silicon. The geometrical taper is de-embedded from both simulation and measured results. The measurements are performed in a 50-Ω system.

IV. 2.25:1 Impedance Transformer

The only realizable transformation ratios of equal-delay TLTs are those that have a rational square root quantity, a proof of which can be found in [15]. An exact 2:1 impedance transformation is therefore not possible. However, an impedance transformation of 2.25:1 can be achieved by connecting only three equal delay transmission lines as shown in Fig. 12(a).

A. Design and Implementation

HFSS is used to implement the transmission line model of the 2.25:1 impedance transformers in the micro-coaxial environment. Since there are additional transmission lines and intra-transformer connections, this design is more challenging than the 4:1 impedance transformer. Fig. 12(b) shows the HFSS model of this transformer. In this design, the lengths of the transmission lines are kept constant, and the intra-transformer connections, as shown on the right side of the figure, are optimized for the lowest possible parasitics given the design rules. Specifically, the separation between the inner conductors in the junctions cannot be less than 80 μm given the gap-to-height ratio of 1:1.2 per layer. Fig. 13 shows the simulated S-parameter comparison between the 2.25:1 impedance transformer shown in Fig. 12(b), and an unoptimized device with parallel straight transmission lines. The resonances that appeared in the unoptimized transformer are mainly due to close proximity of the three transmission lines, and some differences in their lengths. In order to prevent these effects and isolate the transmissions from each other as much as possible, the lines are meandered as shown in Fig. 12(b).

B. Prototype Performance

For measurement the fabricated transformer was released from the silicon and placed on foam. Fig. 14(a) shows the fabricated transformer with the geometrical taper, and (b) shows the sketch of the geometrical taper connecting the 22.22-Ω to the 50-Ω port. This taper, like the one discussed in Section II-B, does not change the 22.2-Ω port impedance significantly due to its short length:

$$Z_{\text{in}} = Z_0 \frac{Z_L + \jmath Z_0 \tan(\beta l)}{Z_0 + \jmath Z_L \tan(\beta l)} = 22.5 + \jmath 5.05\ \Omega \qquad (2)$$

where $Z_0 = 50\ \Omega$, $Z_L = 22.22\ \Omega$, and $l = 0.5$ mm. The measurement was performed with the same setup and calibration standards as discussed in Section II-B. Fig. 15 shows the measured and simulated S-parameter results. A circuit simulator was used to de-embed the effect of geometrical taper on the measured results. For the simulation, the geometrical taper was included and then de-embedded with the same method that was applied to the measured results for fair comparison. The slight shift in the upper frequency limit is due to a small fabrication defect on this particular wafer that has been subsequently fixed; the layer height of the micro-coaxial line varied more than 10%

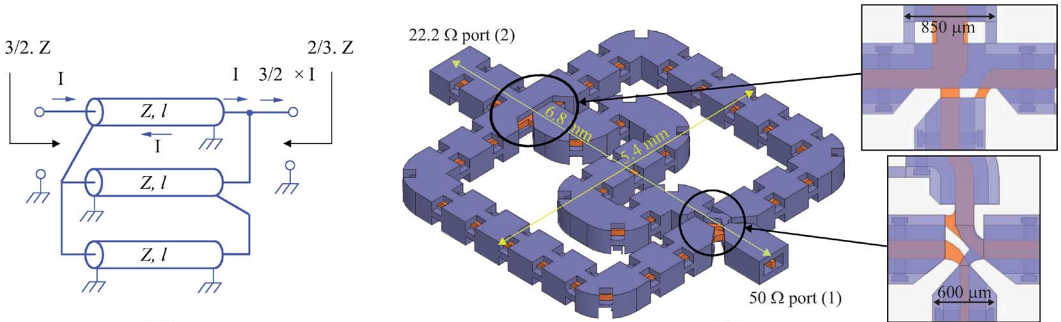

(a) (b)

Fig. 12. (a) Transmission line model of a 2.25:1 impedance transformer. (b) HFSS model of the 2.25:1 impedance transformer; this transformer transforms 50 to 22.2 Ω. The zoomed areas shows the interconnection at the 50-Ω (bottom) junction and 22.2-Ω (top) junction.

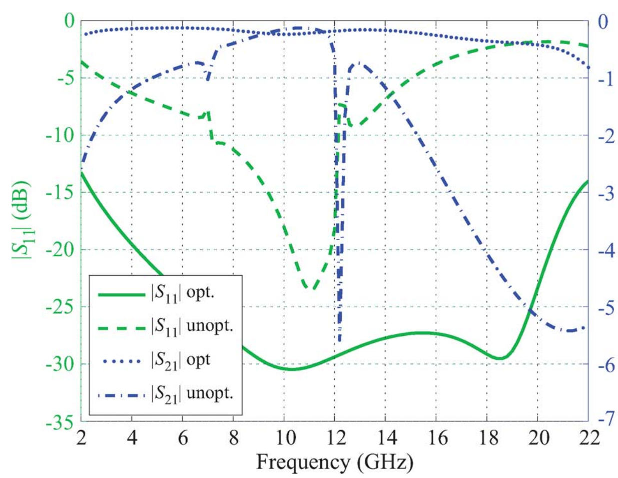

Fig. 13. Simulated S-parameter results comparison for a 2.25:1 impedance transformer with optimized interconnections and isolated transmission lines to a 2.25:1 impedance transformer with unoptimized interconnection and side by side transmission lines.

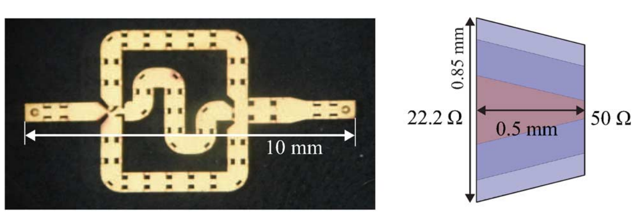

(a) (b)

Fig. 14. (a) Photograph of the 2.25:1 transformer on Si with geometrical taper. (b) Sketch of the geometrical taper connecting the 22.2-Ω line to the 50-Ω line.

resulting in characteristic impedance variations greater than expected.

V. Discussion and Summary

The main application of the impedance transformers is broadband matching, so it is important to compare their performance with commonly used broadband matching networks such as linear and Klopfenstein tapers. For 15-dB return loss at frequencies above 2 GHz, a Klopfenstein and linear taper that match 50 to 12.5 Ω implemented in the micro-coaxial environment are 6 and 10 cm long, respectively. These tapers are more than an order of magnitude longer than the 4:1 impedance

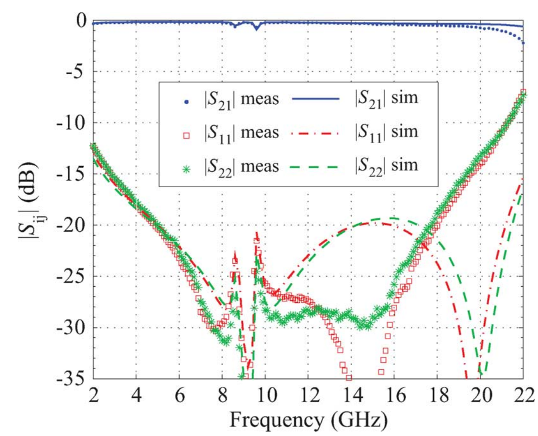

Fig. 15. Simulated and measured results of a 2.25:1 transformer on foam. The measurement is done with a 50-Ω system. The geometrical taper is de-embeded from both simulation and measured results.

transformer presented in this paper, and would therefore be more lossy. Fig. 16 compares the group delay of a Klopfenstein taper and 4:1 transformer designed in micro-coaxial environment and simulated in HFSS. The group delay for both the transformer and the Klopfenstein taper varies about 10 ps between 2 and 5 GHz; however, the transformer group delay is approximately constant above 5 GHz, making it more suitable for pulsed applications.

In summary, in this paper we demonstrated two types of impedance transformers (4:1 and 2.25:1) implemented in wafer-scale fabricated micro-coaxial lines. The 4:1 impedance transformer has 12:1 bandwidth with an upper frequency limit as high as 24 GHz. The effects of different environments around the 4:1 transformer, such as air, cavity, and silicon, were investigated. The cavity backing the transformer increases mechanical stability but does not affect the performance, while when placed on Si, the transformer bandwidth increases at the cost of greater loss. The design method was extended to a 2.25:1 meander-shaped transformer with a 11:1 bandwidth. The measured insertion loss for both transformers in air is less than 1 dB across the bandwidth. One issue associated with this type of transformer is the resonant features that appear in the pass band response due to small discrepancies between the lengths of the transmission lines. The resonance can be removed by placing the transformer on a high dielectric constant material

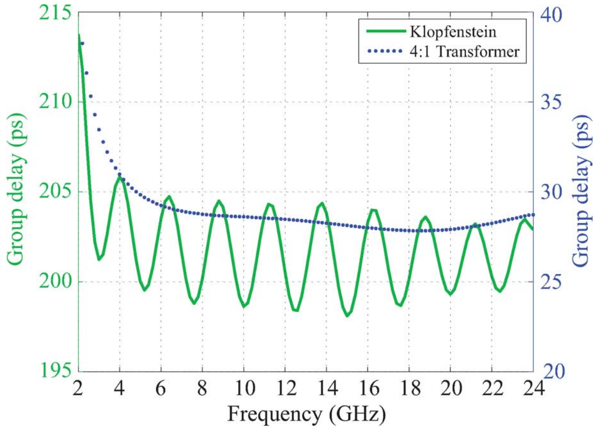

Fig. 16. Group delay for a 6-cm Klopfenstein taper implemented into micro-coaxial environment with 15-dB return loss, and the 4:1 transformer.

(such as Si) in order to decrease the Q of the resonance, at the cost of more loss in the transmission response.

These transformers are attractive for use as matching networks for broadband amplifiers. PolyStrata technology allows for design of other impedance transformation ratios, such as 8:1, with similar bandwidth capabilities. The Guanella impedance transformer design can be implemented as a balun and simultaneously matching network for push–pull designs.

Acknowledgment

The authors would like to thank the Nuvotronics Microfabrication Team, Blacksburg, VA, and Prof. D. Filipović from the University of Colorado at Boulder.

References

[1] G. Guanella, "New method of impedance matching in radio-frequency circuits," *Brown Boveri Rev.*, pp. 327–329, Sep. 1944.

[2] J. Walker, D. Myer, F. Raab, and C. Trask, *Classic Works in RF Engineering Combiners, Couplers, Transformers, and Magnetic Materials*. Norwood, MA: Artech House, 2006, 02062.

[3] R. F. Sobrany and I. D. Robertson, "Ruthroff transmission line transformers using multilayer technology," in *Proc. 33rd Eur. Microwave Conf. 2003*, 2003, pp. 559–562.

[4] J. Sevick, *Transmission Line Transformers*, 4th ed. Raleigh, NC: Scitech Publishing, 2001.

[5] J. Horn and G. Boeck, "Ultra broadband ferrite transmission line transformer," in *IEEE MTT-S Int. Microwave Symp. Dig.*, 2003, vol. 1, pp. 433–436.

[6] M. Engels, R. Jansen, W. Daumann, R. Bertenburg, and F. Tegude, "Design methodology, measurement and application of MMIC transmission line transformers," in *IEEE MTT-S Int. Microwave Symp. Dig.*, 1995, vol. 3, pp. 1635–1638.

[7] K. J. Vanhille, D. L. Fontaine, C. Nichols, D. S. Filipović, and Z. Popović, "Quasi-planar high-Q millimeter-wave resonators," *IEEE Trans. Microw. Theory Tech.*, vol. 54, no. 6, pp. 2439–2446, 2006.

[8] K. Vanhille, D. S. Filipović, C. Nichols, D. Fontaine, W. Wilkins, E. Daniel, and Z. Popović, "Balanced low-loss Ka-band μ-coaxial hybrids," in *Proc. IEEE/MTT-S Int. Microw. Symp. 2007*, 2007, pp. 1157–1160.

[9] M. Lukić and D. Filipović, "Surface-micromachined dual Ka-band cavity backed patch antenna," *IEEE Trans. Antennas Propag.*, vol. 55, no. 7, pp. 2107–2110, 2007.

[10] N. Ehsan, K. Vanhille, S. Rondineau, E. D. Cullens, and Z. B. Popovic, "Broadband micro-coaxial wilkinson dividers," *IEEE Trans. Microw. Theory Tech.*, vol. 57, no. 11, pp. 2783–2789, 2009.

[11] D. Filipović, M. Lukić, Y. Lee, and D. Fontaine, "Monolithic rectangular coaxial lines and resonators with embedded dielectric support," *IEEE Microw. Wireless Compon. Lett.*, vol. 18, no. 11, pp. 740–742, 2008.

[12] K. Vanhille, "Design and characterization of microfabricated three-dimensional millimeter-wave components," Ph.D. dissertation, Univ. of Colorado, Boulder, 2007.

[13] M. Lukić, S. Rondineau, Z. Popović, and S. Filipović, "Modeling of realistic rectangular μ-coaxial lines," *IEEE Trans. Microw. Theory Tech.*, vol. 54, no. 5, pp. 2068–2076, 2006.

[14] N. Ehsan, E. Cullens, K. Vanhille, D. Frey, S. Rondineau, R. Actis, S. Jessup, R. Lender, A. Immorlica, D. Nair, D. Filipović, and Z. Popović, "Micro-coaxial lines for active hybrid-monolithic circuits," in *IEEE MTT-S Int. Microwave Symp. Dig.*, 2009, pp. 465–468.

[15] D. Myer, "Synthesis of equal delay transmission line transformer networks," *Microw. J.*, vol. 35, no. 3, pp. 106–114, Mar. 1992.

Negar Ehsan (S'05–M'10) received the B.S. and M.S. degrees in electrical engineering, with a minor in applied mathematics, in 2006 and the Ph.D. degree in electrical engineering in 2010, all from the University of Colorado at Boulder.

Currently, she is with NASA Goddard Space Flight Center. Her interests include designing passive and active broadband microwave circuits, advanced full-wave electromagnetic modeling techniques, millimeter-wave antenna arrays, radiometers for earth science missions, and THz components for NASA space flight missions.

Dr. Ehsan was the recipient of the 2006 Distinguished Senior Award from the Department of Electrical Engineering, University of Colorado at Boulder.

Kenneth J. Vanhille (S'00–M'07) received the B.S. degree in electrical engineering from Utah State University in 2002, and the M.S. and Ph.D. degrees in electrical engineering from the University of Colorado at Boulder in 2005 and 2007, respectively.

He is currently a Senior Engineer and Program Manager with Nuvotronics LLC, Blacksburg, VA. His technical interests include high-frequency packaging techniques, millimeter-wave components and systems, and antenna design.

Sébastien Rondineau (M'04) received the Ph.D. degree from the University of Rennes 1, France, in 2002.

He was a Research Assistant Professor at the University of Colorado, Boulder until 2008. He was Director of the R&D Department-TSM Antennas, Brazil, from 2008 to 2009 and is currently Director at Solentech, Rio Grande do Sul, Brazil. His research interests include computational electromagnetics, propagation and scattering, antennas and arrays, nonlinear materials, and RF systems.

Zoya Popović (F'02) received the Dipl.Ing. degree from the University of Belgrade, Serbia, in 1985 and the Ph.D. degree from the California Institute of Technology in 1990.

She is a Distinguished Professor and Hudson Moore, Jr., Endowed Chair of Electrical, Computer and Energy Engineering at the University of Colorado, Boulder. She was a Visiting Professor at the Technical University of Munich in 2001. Her research interests include high-efficiency, low-noise and broadband microwave and millimeter-wave circuits, antennas and arrays, radar front ends, and wireless powering for batteryless sensors.

Dr. Popović is the recipient of the 1993 and 2006 Microwave Prizes presented by the IEEE MTT-S for best journal paper. She was the recipient of the 1996 URSI Issac Koga Gold Medal, the Humboldt Research Award from the German Alexander von Humboldt Stiftung and the 2001 HP/ASEE Terman Medal for combined teaching and research excellence.